объединенный
институт
ядерных
исследований
дубна

E2-80-503

D.Yu.Bardin, O.M.Fedorenko, N.M.Shumeiko

RADIATIVE CORRECTIONS TO P-ODD ASYMMETRIES IN DEEP-INELASTIC SCATTERING OF POLARIZED MUONS ON NUCLEONS AT TeV ENERGIES

Submitted to "Journal of Physics"

1980

I. INTRODUCTION

The radiative correction procedure is known to be important in the deep-inelastic lepton-nucleon scattering data processing [1]. In view of CERN experiments on the deep-inelastic muon scattering [2] during last years we have been analysing in detail the radiative corrections (RC) to the processes

$$\ell^{\mp} + N \to \ell^{\mp} + \text{anything} \tag{1}$$

at incident muon energies from 50 GeV up to 300 GeV. We have studied usual electromagnetic corrections and also the corrections due to weak interactions which grow with energy very fast. In particular, in a recent paper [3] based on the Weinberg and Salam theory and on a simple quark-parton model (QPM), we have calculated the one-loop RC to the P-odd asymmetries

$$A^{\mp}(\lambda) = \frac{1}{\lambda} \cdot \frac{d^2\Sigma^{\mp}(\lambda) - d^2\Sigma^{\mp}(-\lambda)}{d^2\Sigma^{\mp}(\lambda) + d^2\Sigma^{\mp}(-\lambda)} \tag{2}$$

and to the charge (or beam conjugation) asymmetry

$$B(\lambda) = \frac{d^2\Sigma^{+}(\lambda) - d^2\Sigma^{-}(-\lambda)}{d^2\Sigma^{-}(\lambda) + d^2\Sigma^{-}(-\lambda)}, \tag{3}$$

where λ is the longitudinal polarization of the initial lepton (antilepton), and $d^2\Sigma^{\mp}$ is the double differential inclusive cross-section of processes (1).

The calculations have been carried out in the approximation

$$m_i^2 \ll I \ll M_W^2 , \tag{4}$$

where I is any invariant of the amplitude, m_i is any mass of scattered particles, M_W is the weak W-boson mass. The l.h.s. of inequality (4) is the necessary condition to apply the QPM; the r.h.s., which is valid at the energies considered in ref.[3], simplifies essentially the resulting formulae.

In this paper, in view of the proposed experiments on deep-inelastic ℓN-scattering at TeV energies[4] we calculate the one-loop RC to asymmetries $A^{\mp}$ and B abandoning the r.h.s. of inequality (4), which does not hold at these energies.

The paper is organized as follows. In the next section we describe in detail the renormalization scheme used for the calculations of the one-loop approximation for the amplitude of lepton-quark scattering. In section 3 we present and discuss the numerical results for asymmetries A^+ and B in the deep-inelastic μN-scattering at incident muon energies E = = 500 GeV, 800 GeV and 30 TeV. (The first two energies lie in the proposed muon beam energy interval for FNAL TEVATRON project, the latter energy is expected to be reached at big world accelerator). In the Appendix all cumbersome formulae are collected.

II. RENORMALIZATION PROCEDURE

For the calculation of the lowest-order radiative corrections, it is necessary to realize the one-loop-level renormalization procedure, all independent parameters of the theory being expressed through the physical (experimentally measured) quantities. In the lepton sector of the Weinberg and Salam theory there are 21+4 independent parameters, where 1 is the number of lepton types ($e, \mu, \tau, \ldots$). At the first step we follow Salomonson and Ueda[5] and choose these parameters as follows: Electron charge e, weak charge g, masses of weak charged boson W and Higgs scalar, M_W and M_χ, and masses of all leptons (physical masses of neutrinos are considered to be zero). However, in contrast with[5], where g is defined as the on-mass-shell constant of the decay $W \to \mu\nu_\mu$, we extract g from the life time of muon, τ_μ, well defined experimental quantity. The g renormalization counterterm is derived from the requirement of zero one-loop RC to the total decay probability of the muon, i.e., we postulate for the renormalized weak interaction constant g_F the tree expression

$$\frac{g_F^4 m_\mu^5}{3 \cdot 2^{11} \pi^3 M_W^4} = \frac{1}{\tau_\mu} = \frac{G_F^2 m_\mu^5}{192 \pi^3} \qquad (5)$$

with the notation of Fermi constant

$$G_F = \frac{\sqrt{2} g_F^2}{8 M_W^2} = \frac{1.0245}{M_P^2} \cdot 10^{-5}. \qquad (6)$$

This step of renormalization procedure is free from unphysical infrared divergences present in the method of Salomonson and Ueda [5] and uses the natural point of fixation of the parameters of the theory, μ-decay constant, which measures the strength of weak processes at small (in the weak interaction scale) transfers. Eq.(5) provides one restriction for three new parameters g_F, M_W and M_χ of the Weinberg and Salam theory. (For the QED charge e in the renormalization scheme [5] the usual expression $e^2 = 4\pi\alpha$ is still valid, $\alpha = 1/137$). It fixes the ratio g_F^2/M_W^2 in the renormalized amplitudes and can be used to exclude W-boson mass, which is not measured up to now. So, we are left with two parameters g_F and M_χ. Instead of g_F we shall use another parameter $\sin\Theta_W^F = e/g_F$. In this case all calculated up to the one-loop corrections observables (e.g., asymmetries) will be the function of two parameters $\sin\Theta_W^F$ and M_χ which are not yet fixed. The computations exhibit, however, a very weak dependence of the asymmetries from the Higgs boson mass; for example, we have observed that variation M_χ within the limits

$$1\ \text{GeV} < M_\chi < 100\ \text{GeV} \qquad (7)$$

gives relative change of asymmetries only within 1%. Therefore, one can take some value for M_χ, say $M_\chi = 100$ GeV, and consider this value as another point of fixation.

Studying asymmetries as functions of $\sin\Theta_W^F$, one can fix the last parameter of the theory. For this purpose we have calculated RC to the SLAC experiment on asymmetry A^-. We used [3] a renormalization scheme, where $\sin\Theta_W$ is derived from eq.(5) and from a physical value of M_W^{ex}, i.e.,

$$\sin\Theta_W^F = \frac{37.3}{M_W^{ex}}\ \text{GeV}. \qquad (8)$$

In this scheme we have observed rather large ($\lesssim 10\%$) RC to A^- in the kinematical region of SLAC experiment. The analysis of formulae showed that these RC come mainly from a near constant contribution of $Z\gamma$-mixing diagrams (this term is of an order of $\ln(M_W^2/m_e^2)$).

So, we have two alternatives: Either to accept the definition (8) for $\sin\Theta_W^F$ and analyze once more the data of experiment by Prescott et al.[6] extracting a corrected value of $\sin\Theta_W$, or to change the definition of $\sin\Theta_W^F$ in order to minimize the RC in the kinematical region of SLAC experiment. The latter is possible because a constant term dominates in this region in the RC. Let us follow the second alternative and define the physical value of $\sin^2\Theta_W^{ex}$ by the equation

$$\sin^2\Theta_W^{ex} = \sin^2\Theta_W^F \cdot \left[1 + \frac{\alpha}{4\pi} \cdot F_R\,(\sin^2\Theta_W^F)\right], \qquad (9)$$

where constant F_R includes the limit at $Q^2 \to 0$ of the $Z\gamma$-mixing diagrams and also the Z-boson self-energy contribution[3]. As a result of redefinition (9) the RC to SLAC experiment become small (see fig.2 in the next section); therefore, the extraction from this experiment of a value of the Weinberg parameter, which has been done by neglecting weak RC, yields practically the same value for $\sin^2\Theta_W^{ex}$ as would be extracted if the latter corrections were taken into account. We shall take for $\sin^2\Theta_W^{ex}$ the mean value of neutrino and asymmetry experiments

$$\sin^2\Theta_W^{ex} = 0.23, \qquad (10)$$

as the last input value in our renormalization scheme.

Eqs.(8) and (9) give the exact prediction for W-boson mass up to one-loop RC

$$M_W = \frac{37.3\ \text{GeV}}{\sin\Theta_W^{ex}}\left[1 + \frac{\alpha}{2\pi} \cdot F_R(\sin^2\Theta_W^{ex})\right]. \qquad (11)$$

At $\sin^2\Theta_W^{ex} = 0.23$ the second term in (11) is about +0.04, i.e., RC increase W-boson from 77.8 GeV to 80.8 GeV.

So, the fixation of the parameter $\sin^2\Theta_W^{ex}$ completes the renormalization procedure in the lepton sector of the Weinberg and Salam theory.

We note that the renormalization procedure realized here differs from those of refs.[7] used to calculate the one-loop RC to the processes $e^+e^- \to \mu^+\mu^-(e^+e^-)$ and is very close to a scheme which is called by Passarino and Veltman[7] to be as "ideal". We are able to realize the "ideal" scheme, because in the previous papers[8] we have calculated the one-loop corrections to the scattering amplitude of any two fermions and also to μ-decay total probability.

To calculate RC to the semileptonic processes (1), it is not enough to complete the renormalization procedure in the lepton sector. Dealing with QPM we include in the Weinberg and Salam theory the doublet of light quarks $\binom{u}{d}$ (we shall work neglecting sea quark contributions). This adds two new input parameters, masses M_u and M_d. We have chosen $M_u = M_d = M$ and investigated the sensitivity of the result to the variation of M. We observed that, if M changes within the limits

$$100 \text{ MeV} < M < 1 \text{ GeV}, \qquad (12)$$

the relative change of asymmetries does not exceed 1% again.

It is obvious that within QPM it is possible to calculate unambiguously only those RC which do not involve quark lines, i.e., RC to the lepton current and self-energy insertions to the exchange quanta virtual lines. But to obtain a finite result within a gauge theory, it is necessary to calculate the total set of the one-loop diagrams including those which involve quark lines. Furthermore we are forced to consider quarks as free particles on mass-shell. It is evident that the estimation of the precision of the results obtained in such a manner is difficult.

The calculations exhibit, however, a rather favourable situation. Let us obtain two radiatively corrected asymmetries. The first one, A_1^+, is derived from the differential cross section $d^2\Sigma_1$; while calculating it we take all one-loop diagrams (fig.1) and realize the whole renormalization program. The second one, $\bar{A}_1^+$, is derived from the corresponding cross section $d^2\bar{\Sigma}_1$, where we leave finite parts of a small number of diagrams only, namely: Lepton bremsstrahlung (diagrams 44 and 45, fig.1), vertex electromagnetic corrections (diagrams of type 22 with additional virtual

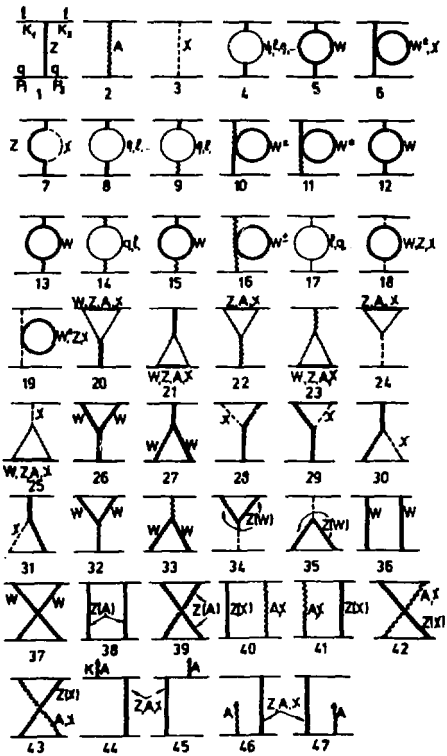

Fig.1.

photon), and finally, vacuum polarization (diagram 14, fig.1) and $Z\gamma$-mixing (diagrams 8 and 9, fig.1). In what follows, this set of diagrams will be referred to as the restricted set of diagrams. The formulae describing the contributions of these diagrams to the considered cross section $d^2\Sigma_1$ are given in the Appendix.

The computations show that the assymmetries $A_1^{\mp}$ are practically the same as $\bar{A}_1^{\mp}$ (see figures in the next section). This means that the radiative effect can be approximated very well only by the restricted set of diagrams, i.e., it is free of the QPM uncertainties.

Due to this reason and cumbersome representation of the formulae for the total set of diagrams of fig.1, they are not given in the Appendix; thus we restrict ourselves only to the presentation and discussion of numerical results corresponding to the total set of diagrams.

III. DISCUSSION OF RESULTS

In figures 2 and 3-7 we show the results of computations of the asymmetry A^- for SLAC experiment and asymmetries A^+ and B for the deep-inelastic muon-nucleon scattering in TeV energy range. These curves, corresponding to the scattering on an isoscalar nucleon, have been computed at $\sin^2\Theta_W^{ex} = 0.23$,

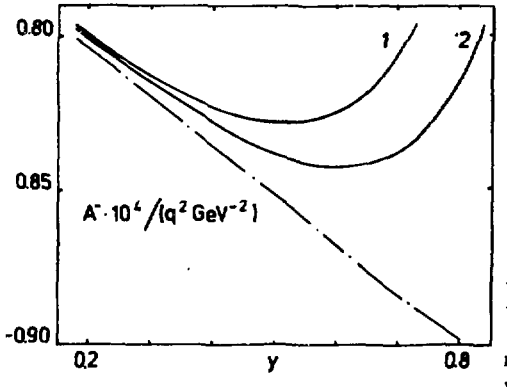

Fig. 2

M = 0.33 GeV, for the parton spectra the parametrization of Barger and Phillips /9/ being used. All asymmetries are shown as functions of the scaling variable y at fixed Q^2. The numbers, placed close to the curves in figures show the values of Q^2 in units GeV^2. The solid lines represent asymmetries A_1^+ calculated with the total set of diagrams, dotted lines correspond to asymmetries $\bar{A}_1^+$ derived from the restricted set. As a measure of the radiative effect, we take the quantity

$$\delta_{A(B)} = \frac{A_1(B_1) - A_0(B_0)}{A_0(B_0)}, \quad (13)$$

where $A_0(B_0)$ is the Born asymmetries calculated with diagrams 1 and 2, fig.1.

From fig.2 we conclude that RC to A^- at SLAC kinematics are really small in our renormalization scheme. This permits us to consider the mean experimental value for $\sin\Theta_W^{ex}$ as an input for our calculations.

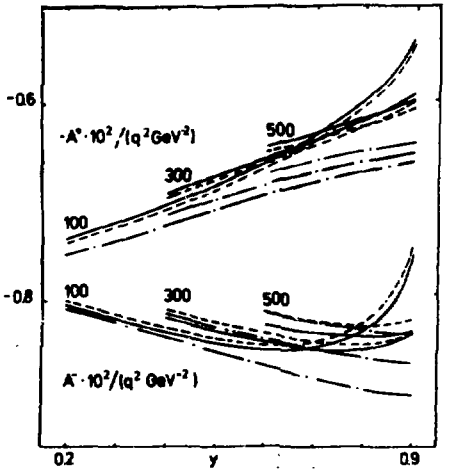

Fig.3

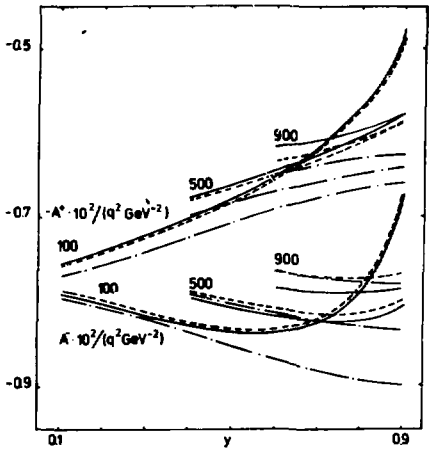

Fig. 4

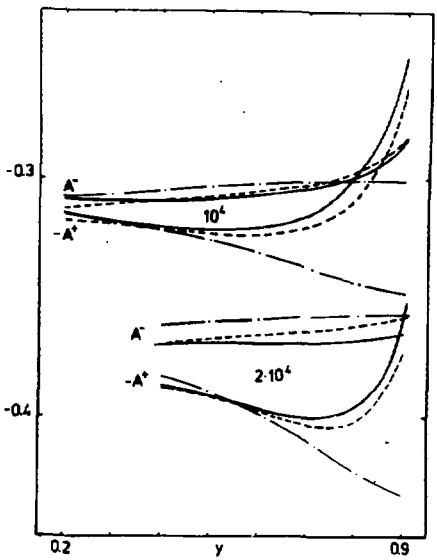

Fig 5

From figs.3-7 one can see that both asymmetries and the radiative effects depend mainly on Q^2 and y but not on energy at fixed Q^2 and y . At energies E = 500--800 GeV the most prominent is the RC δ_B reaching dozens of per cent, RC $\delta_A^{\mp}$ do not exceed 10% in the greater part of the kinematical region but grow very fast at small Q^2 when y goes to unity. This is the effect of the hard photon bremsstrahlung.

One can see also that in the major part of the kinematical region, excluding high Q^2 domain, the radiative effect for the asymmetries $A^{\mp}$ is well approximated by the restricted set of diagrams. The contributions of other diagrams are small or cancel each other.

For the asymmetry B the radiative effect cannot be calculated using the restricted set of diagrams, because of the large contributions to B coming from diagrams with 2γ-exchange (diagrams of the type 38 and 39, fig.1) and from interference of diagrams 44-45 with 46-47. These contributions, changing the sign from 1^-N to 1^+N - scattering are of the order α but are not suppressed by the factor Q^2/M_W^2 as the other terms are. For this reason their relative contributions to B depend on

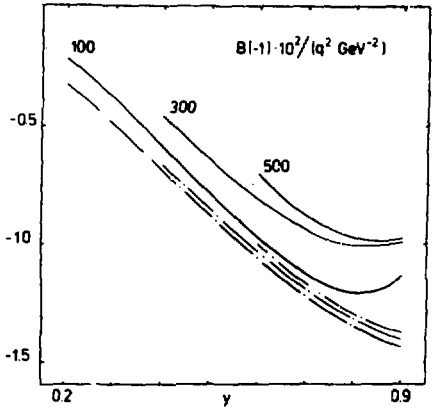

Fig.6

Q^2 and can be large, especially at low energies. Just these terms dominate in the RC to B at E = 500--800 GeV (see fig.6). However, at $Q^2 \simeq M_W^2$ these terms approach to the other one-loop contributions to B. As a consequence of this fact, the RC both to A and B exhibit similar behiviour at TeV energies.

In conclusion we emphasize that in the considered energy range the usage of the r.h.s. approximation (4) would yield quite an incorrect result even up to an order of magnitude and sign. At these energies Z-exchange squared contributions are not negligible as compared to the usual $Z\gamma$-interference terms.

The authors are indebted very much to M.Klein and I.A.Savin for valuable discussions.

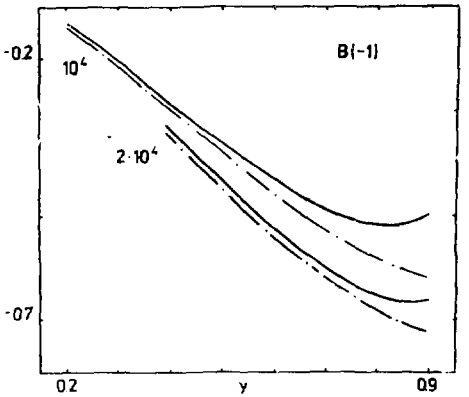

Fig 7

APPENDIX

Here we list the contributions to the cross section $d^2\bar{\Sigma}_1$ from the diagrams belonging to the restricted set.

I. Vertex electromagnetic corrections to the lepton current (diagrams of the type of 20 and 22 fig.1 with additional vartual photon)

$$d^2\Sigma_V = \frac{\alpha}{\pi}\left(-2 + \frac{3}{2}\ln\frac{V}{m^2}\right) d^2\Sigma_0 . \quad (A.1)$$

Here

$$d^2\Sigma_0 = d^2\Sigma_0^A + d^2\Sigma_0^{ZA} + d^2\Sigma_0^Z, \tag{A.2}$$

$$\frac{d^2\Sigma_0^A}{dx\,dy} = K\cdot[1+(1-y)^2]\sum_i x f_i(x)\,Q_i^2, \tag{A.3}$$

$$\frac{d^2\Sigma_0^{ZA}}{dx\,dy} = K\cdot\eta\cdot\sum_i x f_i(x)\,|Q_i|\cdot[\Theta_i^+ + (1-y)^2\Theta_i^-], \tag{A.4}$$

$$\frac{d^2\Sigma_0^Z}{dx\,dy} = K\cdot\eta^2\cdot\sum_i x f_i(x)\,[\Lambda_i^+ + (1-y)^2\Lambda_i^-], \tag{A.5}$$

where

$$K = \frac{2\pi\alpha^2 S_N}{Y^2}, \quad \eta = \frac{Y}{4\sin^2\Theta_W^{ex}(\bar{M}_W^2 + Y\cos^2\Theta_W^{ex})}, \quad Y \equiv Q^2, \tag{A.6}$$

$$\Theta_i^{\pm} = \frac{1}{2}\cdot[b_i\,(a+s\lambda) \mp (s+a\lambda)], \tag{A.7}$$

$$\Lambda_i^{\pm} = \frac{1}{16}(1+b_i^2)(1+a^2+2as\lambda) \mp \frac{1}{8}b_i[(1+a^2)\lambda + 2as], \tag{A.8}$$

$s = -1$ for 1^-N -scattering, and $s = +1$ for 1^+N -scattering. In formulae (A.1)-(A.2) the following notation is used $S_N = 2M_N E$, M_N is the nucleon mass, m is the mass of a scattering lepton, E is its energy in the lab. system, Q_i is the i-th quark charge, $f_i(x)$ is the i-th quark momentum distribution, $a = 1-4\sin^2\Theta_W^{ex}$, $b_i = 1-4|Q_i|\sin^2\Theta_W^{ex}$, $\bar{M}_W = 37.3/\sin\Theta_W^{ex}$. In summing over parton types i in (A.3)-(A.5) and below we take into account the *contributions from* valence u - and d - quarks only.

II. Vacuum polarization by fermions (diagram 14 of fig.1)

$$d^2\Sigma_P = \frac{\alpha}{\pi}\mathcal{P}(Y)\cdot(d^2\Sigma_0^A + \frac{1}{2}d^2\Sigma_0^{ZA}), \tag{A.9}$$

$$\mathcal{P}(Y) = \frac{2}{3} \sum_f Q_f^2 \left(-\frac{5}{3} + \ln \frac{Y}{m_f^2}\right). \qquad (A.10)$$

Summing (A.10) extends over all charged fermions ($e, \mu, \tau, q, \ldots$) which can appear in vacuum loops. In numerical calculations we take into account only the most important contributions from the lightest fermions, namely from e, μ, u and d -loops. Leaving u -and d -loops we approximate to some extent the contribution of the hadron vacuum polarization.

III. $Z\gamma$-mixing through fermion loops (diagrams 8 and 9 fig.1)

$$\frac{d^2\Sigma_M}{dx\,dy} = \frac{\alpha^3 S_N \sin^2\Theta_W^{ex}}{Y^2} \cdot \eta \cdot T_0 \cdot D(Y) \sum_i x f_i(x) |Q_i| \left[-(b_i + a|Q_i|) + \lambda(R(y) - \right.$$

$$\left. -s|Q_i|) \right] + \frac{\alpha^3 S_N \sin^2\Theta_W^{ex}}{4Y^2} \cdot \eta^2 \cdot T_0 \cdot D(Y) \sum_i x f_i(x) \left\{ -\left[b_i (1 + a^2 + 2as\lambda) |Q_i| + \right.\right.$$

$$\left.\left. + (1 + b_i^2)(a + s\lambda) \right] + R(y) \left[|Q_i| \cdot (2as + (1 + a^2)\lambda) + 2 b_i (s + a\lambda) \right] \right\}, \qquad (A.11)$$

$$R(y) = \left[1 - (1-y)^2 \right] / T_0 , \qquad T_0 = 1 + (1-y)^2 , \qquad (A.12)$$

$$\mathcal{P}(Y) = \frac{1}{3} \sum_f \left(4 Q_f^2 - \frac{|Q_f|}{\sin^2\Theta_W^{ex}}\right)\left(-\frac{5}{3} + \ln \frac{Y}{m_f^2}\right). \qquad (A.13)$$

IV. Lepton Bremsstrahlung (diagrams 44 and 45 fig.1).

For the contribution of these diagrams to the differential cross section $d^2\Sigma_1$, we use the following representation

$$d^2\Sigma_R = \frac{\alpha}{\pi} \kappa\, d^2\Sigma_0 + d^2\Sigma_m + d^2\Sigma_R^F , \qquad (A.14)$$

where

$$\frac{d^2\Sigma_m}{dx\,dy} = \frac{\alpha}{\pi} J(Y) \frac{d^2\Sigma_0}{dx\,dy} \Big|_{x f_i(x) \to \int_x^1 \frac{\xi f_i(\xi) - x f_i(x)}{\xi - x} d\xi}, \tag{A.15}$$

$$\kappa = -\frac{1}{2}\ln^2(1-y) - \frac{1}{2} J(Y) \ln \frac{x^2(1-y)}{y^2(1-x)^2}, \tag{A.16}$$

$$J(Y) = 2\cdot(-1 + \ln \frac{Y}{m^2}), \tag{A.17}$$

and the last term in eq. (A.14), we have expressed as the sum

$$\frac{d^2\Sigma_R^F}{dx\,dy} = \alpha^3 y \sum_i \int_x^1 f_i(\xi) \frac{d\xi}{\xi} \cdot (Q_i^2 \cdot \sigma_i^A + \eta |Q_i| \sigma_i^{ZA} + \eta^2 \sigma_i^Z). \tag{A.18}$$

The first term in eq. (A.18) is the contribution to $d^2\Sigma_R^F$ from the square of the sum of diagrams 44 and 45 with virtual photon exchange

$$\sigma_i^A = \Phi_i(S; X) + \Phi_i(-X; -S), \tag{A.19}$$

where

$$\Phi_i(S;X) = -\frac{1}{S_Y} \ell_A^i + \frac{1}{S_X} \ell_t^i - \frac{1}{Y}\Big[J(Y) + \frac{V\cdot T}{SXY}\Big] - \frac{2}{XY}\Big(S - \frac{Y}{2} - \frac{T}{Y}\Big) \ell_X^i, \tag{A.20}$$

$$\ell_A^i = \ln \frac{S_Y^2}{m^2 r_i}, \quad \ell_t^i = \ln \frac{(V S_X + M_i^2 Y)^2}{M_i^2 Y^2 r_i}, \quad \ell_X^i = \ln \frac{X^2}{m^2 M_i^2}, \tag{A.21}$$

$$r_i = V + M_i^2, \quad V = S_X - Y, \quad S_X = S - X, \quad Y = xy\,S_N, \quad S = \xi S_N, \quad X = \xi S_N (1-y),$$
$$S_Y = S - Y, \quad X_Y = X + Y, \quad T = S^2 + X^2. \tag{A.22}$$

The second term in (A.18) corresponds to the interference of bremsstrahlung diagrams 44 and 45 with γ-and Z-exchanges

$$\sigma_i^{ZA} = \Theta_i^+ F_i(S;X) + \Theta_i^- F_i(-X;-S), \tag{A.23}$$

$$F_i(S;X) = \frac{2S_X}{Y^2} - \frac{1}{Y}(1+\frac{S_1}{Y})J(Y) + \frac{Y_Z}{Y S_X}\ell_t^Z + \frac{2S(M_Z^2 - X)}{Y \cdot D_X} + \frac{2}{Y}[\frac{SX - X_Y M_Z^2}{D_S}] -$$

(A.24)

$$- \frac{S^2 + X_Y^2}{Y \cdot Y_Z} L_S^Z - \frac{1}{Y}[2X_Y - \frac{S^2 + X_Y^2}{Y_Z}] L_X^Z + \frac{Y_Z}{Y \cdot S_Y}[S_Y L_X^Z - \ell_A^i].$$

Here and below $D_S = SY + X_Y M_Z^2$, $D_X = -D_S(S \to -X)$,

$$S_1 = S + X, \quad \ell_t^Z = \ln \frac{V \cdot S_Z + M_i^2 Y_Z}{M_Z^2 V + M_i^2 Y_Z}, \quad S_Z = S_X + M_Z^2, \quad Y_Z = Y + M_Z^2, \qquad (A.25)$$

$$L_S^Z = \frac{Y_Z}{D_S} \ln \frac{D_S^2}{m^2[M_i^2 Y^2 + M_Z^2(VS_X + 2M_i^2 Y) + M_Z^4 r_i]}, \qquad (A.26)$$

$$L_X^Z = -L_S^Z (S \to -X), \qquad (A.27)$$

$$M_Z^2 = \bar{M}_W^2 / \cos^2 \Theta_W^{ex}. \qquad (A.28)$$

Finally, the last term in (A.18) is the contribution to $d^2\Sigma_R^F$ from the diagrams 44-45 with Z-exchange bremsstrahlung

$$\sigma_i^Z = \Lambda_i^+ M_i(S;X) + \Lambda_i^- M_i(-X;-S), \qquad (A.29)$$

$$M_i(S;X) = -\frac{1}{Y}(1+\frac{S_1}{Y})J(Y) + \frac{Y_Z^2}{Y^2 S_Y}\cdot[S_Y L_X^Z - \ell_A^i] + \frac{V}{Y^2}(1 - \frac{V}{S_Z}) -$$

$$- \frac{Y_Z}{Y^2}(1 - \frac{Y_Z}{S_X}\ell_t^Z) + \frac{S^2 + X_Y^2}{Y^2}[\frac{M_Z^2}{Y_Z} - \frac{SY}{D_S}] L_S^Z + \{\frac{1}{Y_Z}[\frac{T}{Y} - Y +$$

$$+ \frac{2X_Y \cdot V \cdot M_Z^2}{D_X}] - \frac{M_Z^2}{Y \cdot D_X}\cdot[V M_Z^2 + X \cdot S_1 + \frac{SX^2}{Y} + S_Y(X + 2Y + \frac{S^2}{Y})]\} L_X^Z +$$

$$+\frac{Y_Z^2}{D_X^2}\left[\frac{2S^2}{Y_Z}+\frac{X\cdot S_1\cdot M_Z^2}{D_S}-\frac{1}{Y^2}\left(XY-\frac{SVM_Z^2}{S_Z}\right)\frac{X^2+S_Y^2}{Y_Z}\right]+$$

$$+\frac{1}{Y\cdot D_X}\left\{M_Z^2(4X+Y)-2X\,S_1+\frac{XM_Z^2[2SV+Y\cdot Y_Z]}{D_X}\right\}+$$

$$+\frac{Y_Z^2}{D_S^2}\cdot\left[-\frac{2X^2}{Y_Z}+\frac{S\cdot S_1\cdot M_Z^2}{D_X}+\frac{1}{Y^2}\left(SY-\frac{X\cdot V\cdot M_Z^2}{S_Z}\right)\frac{S^2+X_Y^2}{Y_Z}+\right.$$

$$\left.+\frac{2}{Y^2}\left(XY-\frac{SVM_Z^2}{S_Z}\right)\left(X_Y-\frac{Y\cdot S_1}{Y_Z}-\frac{Y_Z}{2}\right)\right]. \qquad (A.30)$$

Summing I to IV we obtain the resulting expression for $d^2\bar{\Sigma}_1$ which is used for the calculation of asymmetries

$$d^2\bar{\Sigma}_1 = d^2\Sigma_0 + d^2\Sigma_V + d^2\Sigma_P + d^2\Sigma_M + d^2\Sigma_R.$$

REFERENCES

1. Mo L.W., Tsai Y.S. Rev.Mod.Phys., 1969, 41, p.205.
2. Glifft R. et al. CERN (SPSC), 1974, 74-78, p.18.
   Krienen F. et al. CERN (SPSC), 1974, 74-79, p.19.
3. Бардин Д.Ю., Федоренко О.М., Шумейко Н.М. ЯФ, 1980, 32, с.782.
4. Wilson R.R. Rev.Mod.Phys., 1979, 51, p.259.
5. Solomonson P., Ueda Y. Phys.Rev., 1975, D8, p.3612.
6. Prescott C.Y. et al. Phys.Lett., 1978, 77B, p.347.
7. Passarino G., Veltman M. Nucl.Phys., 1979, B160, p.151.
   Consoli M. Nucl.Phys., 1979, B160, p.208.
8. Бардин Д.Ю., Федоренко О.М. ОИЯИ, Р2-11413, Р2-11414, Дубна, 1978.
9. Barger V., Phillips P.J.M. Nucl.Phys., 1974, B73, p.268.

Received by Publishing Department
on July 14 1980.